Proceedings of the ASME 2017 International Design Engineering Technical Conferences and Computers and Information in Engineering Conference
IDETC/CIE 2017
August 6-9, 2017, Cleveland, Ohio, USA

DETC2017-67373

DESIGN AND INTEGRATION OF A TWO-DIGIT EXOSKELETON GLOVE

Eric Refour
Robotics and Mechatronics Lab
Mechanical Engineering Dept.
Virginia Tech
Blacksburg, VA, USA
erefour@vt.edu

Bijo Sebastian
Robotics and Mechatronics Lab
Mechanical Engineering Dept.
Virginia Tech
Blacksburg, VA, USA
bijo7@vt.edu

Pinhas Ben-Tzvi
Robotics and Mechatronics Lab
Mechanical Engineering Dept.
Virginia Tech
Blacksburg, VA, USA
bentzvi@vt.edu

ABSTRACT

This paper presents the design and integration of a two-digit exoskeleton glove. The proposed glove is designed to assist the user with grasping motions, such as the pincer grasp, while maintaining a natural coupling relationship among the finger and thumb joints, resembling that of a normal human hand. The design employs single degree of freedom linkage mechanisms to achieve active flexion and extension of the index finger and thumb. This greatly reduces the overall weight and size of the system making it ideal for prolonged usage. The paper describes the design, mathematical modeling of the proposed system, detailed electromechanical design, and software architecture of the integrated prototype. The prototype is capable of recording information about the index finger and thumb movements, interaction forces exerted by the finger/thumb on the exoskeleton, and can provide feedback through vibration. In addition, the glove can serve as a standalone device for rehabilitation purposes, such as assisting in achieving tip or pulp pinch. The paper concludes with an experimental validation of the proposed design by comparing the motion produced using the exoskeleton glove on a wooden mannequin with that of a natural human hand.

1. INTRODUCTION

Over the past few decades, exoskeletons and haptic gloves have emerged in popularity within the fields of virtual reality (VR) and medical applications. In the realms of VR, exoskeletons and haptic gloves are used to create realistic experiences by generating tactile responses to reflect the sensation of the user touching an object [1]–[3]. Within the medical field, exoskeleton gloves are used in numerous ways, such as being an assistive tool for tele-operated surgeries or serving as a rehabilitation tool for people who suffer from paralysis in the hand and/or fingers [4]–[6]. Unfortunately, many of these commercial gloves are expensive and require complex equipment, making them unwieldy and less portable for activities of daily living (ADLs).

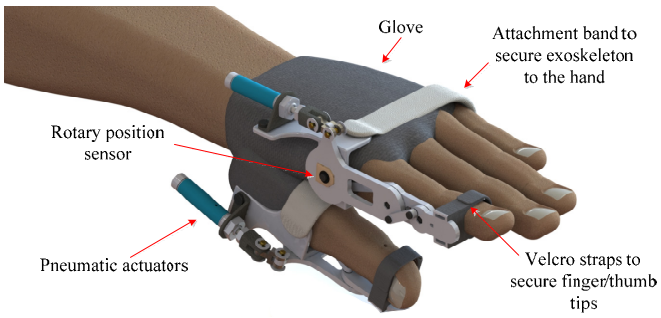

Figure 1. Proposed design.

There have been two main approaches for designing exoskeleton gloves throughout the years. Many researchers use the traditional approach towards building an exoskeleton glove, which involves using rigid links and joints to apply forces to the corresponding joints of the human hand to provide assistance with flexion and extension [7]–[19]. Most of these exoskeleton gloves are designed with the link frames placed on top of the fingers and hand instead of alongside the fingers. This is primarily due to the fact that the size of the link frames exceeds the available space between fingers. The major drawback of this concept is that it results in a bulky and heavy glove, which can result in increased user fatigue during prolonged operation.

The second commonly used approach towards designing exoskeleton gloves is to replace the rigid mechanisms with softer materials. This approach focusses on using a tendon-driven design [20]–[23] or elastic polymers as inflatable membranes, which expand to achieve the desired bending

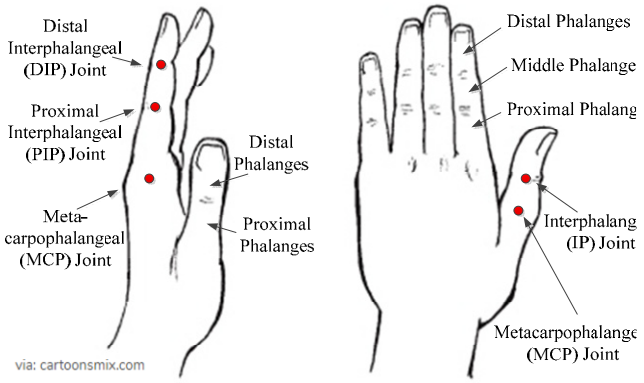

Figure 2. Anatomy of the human hand.

profiles similar to that of human fingers [24]–[26]. Unfortunately, both designs have their share of disadvantages. The soft gloves driven by tendon cables have the following drawbacks: discomfort produced by the pre-tensioning of the cables, loss in efficiency caused by friction along the tendon path, and the creation of shear forces applied onto the soft material by the tendons during flexion and extension. These factors together hinder effective force transmission in tendon driven systems thereby decreasing their repeatability. On the other hand, the soft inflatable gloves are challenged by their inability to provide natural flexions and extensions profiles for the human finger and are therefore limited to only achieving the basic configurations of fully open or closed fist.

The aim of this paper is to present an exoskeleton glove designed to overcome the previously mentioned drawbacks of traditional hard and soft exoskeleton gloves. The exoskeleton glove is intended to be general purpose, possessing the ability to serve as a medical device or virtual reality haptic glove. As a proof of concept for the proposed glove design shown in Fig. 1, a two-digit (index finger and thumb) prototype was developed and its functionality was validated through experimental analysis. For the experimental analysis, one of the potential applications of the full glove is explored; an assistive glove providing support for disabled teens/adults. The rest of the paper is organized as follows: the conceptual design and mathematical modeling are described in Section 2 while Section 3 covers the detailed electromechanical design of the prototype. Section 4 presents the integration of the two-digit prototype and Section 5 discusses the experimental results. Finally, Section 6 concludes the paper with proposal for future work.

2. MECHANICAL DESIGN

In order to overcome the shortcomings of existing systems, the proposed exoskeleton glove was designed to satisfy two primary goals: 1) The weight and size of the total system should be small enough for it to be used in ADL's without fatigue and 2) The system should be capable of producing natural joint angles on the fingers and thumb during flexion and extension movements.

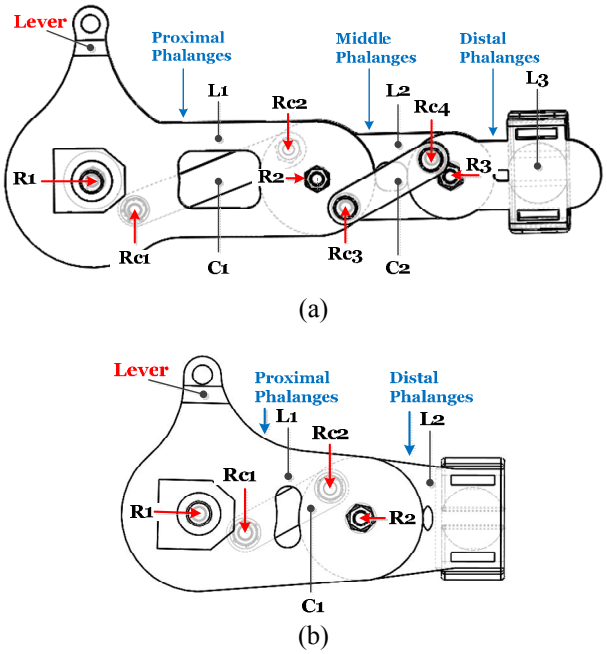

Figure 3. (a) Design of the index finger mechanism, (b) Design of the thumb mechanism.

Fig. 2 illustrates the major joints on a human hand. The fingers consist of three main joints, the metacarpophalangeal (MCP), proximal interphalangeal (PIP), and distal interphalangeal (DIP) joints, while the thumb contains the interphalangeal (IP) and MCP joints. In order to design an exoskeleton glove that satisfies the above mentioned goals, existing studies on human grasping motions, such as the common pinch, were reviewed [27]–[29]. In [30], experiments were performed to measure the joint angles for the index finger and thumb during a tip-pinch motion. The data showed that with a tip-pinch force of 100g and a pulp distance of 1cm, the index finger yielded joint angles of 49.1° (SD 9.5°), 41.0° (SD 10.7°), and 38.5° (SD 6.8°) for the MCP, PIP, and DIP joints respectively while the thumb yielded 12.8° (SD 9.4°), and 21.8° (SD 7.8°) for the MCP and IP joints. This data was used as a reference to design the exoskeleton glove.

A major conclusion drawn from these studies is the existence of inherent coupling of the human finger (MCP, PIP and DIP joints) and thumb (IP and MCP joints). As a result of this coupling, the human fingers and thumbs essentially behave as single DOF systems while flexing and extending to perform common grasping motions. Making use of this factor in the design reduces the number of actuators needed, which in turn reduces the overall size and weight of the system.

The conceptual design for the proposed glove is inspired from the USC/Belgrade Robotic Hand [31]. The coupling mechanism used in this robotic hand was proven successful, so the approach was to adopt a similar coupling mechanism and modify it for suitable use in an exoskeleton glove. The proposed design for the glove mechanism consists of planar links that are connected by revolute joints, as detailed in Fig. 3.

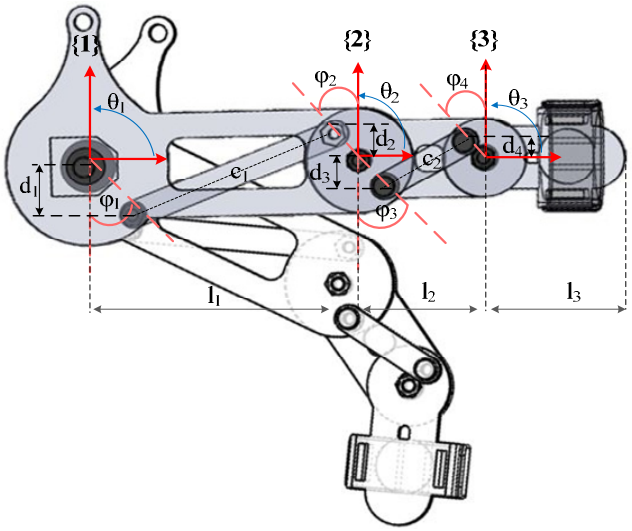

Figure 4. Index mechanism showing two configurations and the design parameters for kinematic modelling. The relaxed configuration is shown in gray, while the black & white schematic shows a flexion configuration

The basic structure of the mechanism for the index finger is composed of links L_1, L_2, and L_3, which correspond to the proximal, middle, and distal phalanges of the finger respectively, as shown in Fig. 3. These three links are connected through three revolute joints, R_1, R_2, and, R_3. Specifically, links L_i and L_{i+1} are connected through revolute joint R_{i+1}. The constraint links C_1 and C_2 are used to produce the coupling relationship between the L_i links. Constraint link C_1 connects link L_2 to a fixed base frame (ground) by revolute joints Rc_1 and Rc_2, while constraint link C_2 connects links L_1 to L_3 through joints Rc_3 and Rc_4. The thumb mechanism is similar, containing only links L_1 and L_2, which are connected by revolute joint R_2. The coupling action for the thumb mechanism is achieved by the constraint link C_1, which connects link L_2 to the base frame through the revolute joints Rc_1 and Rc_2. The assembly of the mechanisms shown in Fig. 3, can be summarized in the following steps:

- Link L_1 is connected to the ground at joint R_1
- Link L_1 is connected to link L_2 at joint R_2
- Link L_2 is connected to link L_3 at joint R_3 *
- Constraint link C_1 connects to the ground at constraint joint Rc_1 and to link L_2 at constraint joint Rc_2
- Constraint link C_2 connects to link L_1 at constraint joint Rc_3 and to link L_3 at constraint joint Rc_4 *

Note: * only applied for the finger mechanism and not for the thumb mechanism.

The flexion and extension motions are achieved when a rotary motion is applied at joint R_1 by pushing and pulling on the lever of link L_1 respectively. This causes link L_1 to bend and as it bends, the constraint links C_1 and C_2 translates the motion along to links L_2 and L_3, as illustrated in Fig. 4. This collectively provides the coupling motion that reflects the natural flexion and extension of a human finger.

2.1 Kinematic Modeling:

Before a detailed mechanical design of the exoskeleton glove could be created, the lengths of various links and positioning of revolute joints had to be determined based on the general dimensions of a human hand and the joint angles desired to be achieved in reference to [30]. To this extent a kinematic modeling of the mechanism was done. The modelling was done taking into consideration the following design parameters (illustrated in Fig. 4):

- l_i- length of link L_i
- c_i- length of constraint link C_i
- θ_i- joint angle of link L_i
- d_i- the radial distance of constraint joint Rc_i, expressed in local coordinates
- φ_i- the angle made by constraint joint Rc_i in respect to the vertical Y axis

The finger mechanism has three DOF, which can be expressed in the coordinates corresponding to the three planar links: $[(x_1, y_1, \theta_1), (x_2, y_2, \theta_2), \text{and} (x_3, y_3, \theta_3)]$, as shown in Fig. 4. The thumb mechanism on the other hand has two DOF: $[(x_1, y_1, \theta_1)\ and (x_2, y_2, \theta_2)]$. For the single DOF mechanism for the index finger, establishing θ_1 as the input variable in the modeling yields the following eight constraint equations:

$$
\begin{aligned}
x_1 &= 0 \\
y_1 &= 0 \\
x_2 &= x_1 + l_1 \cos\theta_1 \\
y_2 &= y_1 + l_1 \sin\theta_1 \\
x_3 &= x_2 + l_2 \cos\theta_2 \\
y_3 &= y_2 + l_2 \sin\theta_2 \\
c_1^2 &= [x_2 + (-d_2 \sin\varphi_2 \cos\theta_2) - d_2 \cos\varphi_2 \sin\theta_2 - d_1 \sin\varphi_1]^2 \\
&\quad + [y_2 + (-d_2 \sin\varphi_2 \sin\theta_2) + d_2 \cos\varphi_2 \cos\theta_2 - d_1 \cos\varphi_1]^2 \\
c_2^2 &= [x_1 + (l_1 + d_3 \sin\varphi_3 \cos\theta_1) - (-d_3 \cos\varphi_3 \sin\theta_1) \\
&\quad - x_3 - (-d_4 \sin\varphi_4 \cos\theta_3) + d_4 \cos\varphi_4 \sin\theta_3]^2 \\
&\quad + [y_1 + (l_1 + d_3 \sin\varphi_3 \sin\theta_1) - (-d_3 \cos\varphi_3 \cos\theta_1) \\
&\quad - y_3 - (-d_4 \sin\varphi_4 \sin\theta_3) + d_4 \cos\varphi_4 \cos\theta_3]^2
\end{aligned}
\qquad (1)
$$

For the above equations, the constraint links C_i are considered to be absolute distance constraints. For the kinematic model, the link lengths L_i were set to general dimensions of a human hand. The other design parameters were estimated using a MATLAB simulation so that the joint angles achieved by the mechanism matched with the joint angles of a natural human finger. The design procedure for the thumb

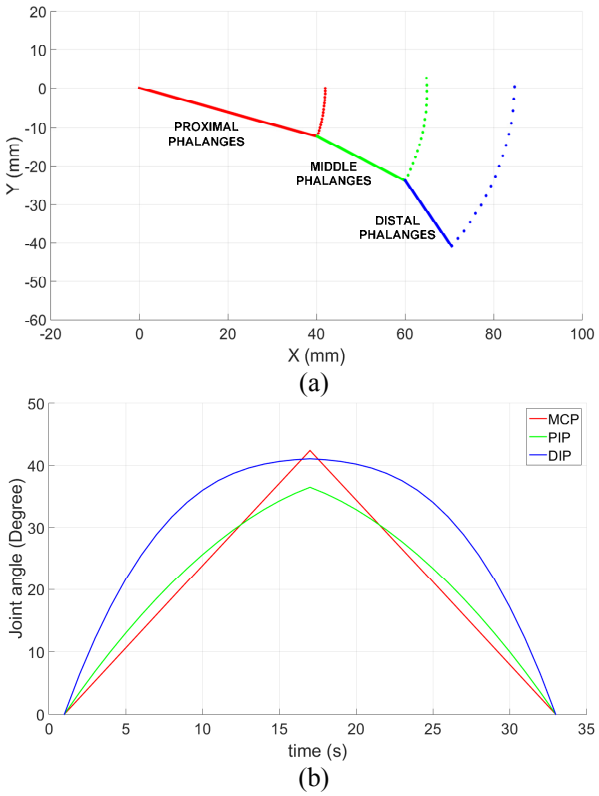

Figure 5: (a) Simulation of the desired index finger trajectory starting at the origin of (0,0), (b) Index finger joint angles.

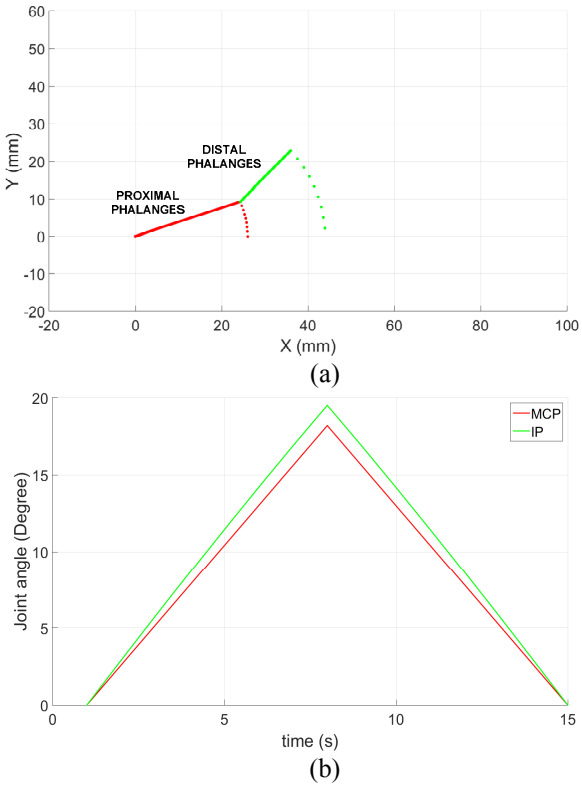

Figure 6: (a) Simulation of the desired thumb trajectory starting at the origin of (0,0), (b) Thumb joint angles.

mechanism follows the same steps, but with only two main links L_i and one constraint link C_i.

Fig. 5 and Fig. 6 each present the kinematic simulation results using the estimated design parameters. The index finger trajectory can provide maximum angles of 43°, 41°, and 37° for the MCP, PIP, and DIP joints respectively, while the thumb trajectory offers MCP and IP angles of 19° and 17° respectively. The simulated trajectories reflect the natural joint relationship of the index finger and thumb during the 100g tip-pitch motion, shown in Fig. 5a and Fig 6a. respectively. These modelling results confirm that the each mechanism is capable of enforcing joint angles resembling that of a natural human hand.

3. ELECTRO-MECHANICAL DESIGN

3.1 Actuation:

To achieve flexion and extension motions with adequate speed and force, Bimba double acting pneumatic actuators were used for the index finger and thumb mechanisms of the exoskeleton glove. With these actuators, the glove can complete flexion and extension motions within 1s with a force of 10N. The complete pneumatic system consists of an air compressor (150 PSI), a 0.5 gallon air reservoir, a pressure regulator, air tubing, and SMC solenoid valves, which controls the air flow into the pneumatic actuators.

3.2 Sensors:

For absolute position sensing, Bourns rotary encoders were placed on each of the finger and thumb mechanisms at the R_1 joints, which correspond to the MCP joints on the human hand. The readings from the electrical encoders corresponds to the angular position of the L_1 links of the finger and thumb mechanisms. A digital protractor was used to manually calibrate the encoder values into angle measurements. The remaining joint angles of the PIP and DIP joints of the index finger and the IP joint of the thumb are calculated using the kinematic model of the mechanism. Using the kinematic model the position of the final link corresponding to the distal phalanges of the finger and thumb, can also be calculated.

Force sensitive resistors (FSR) by Interlink Electronics were used to measure the amount of force being applied on the index finger and thumb by the exoskeleton frames during grasping. These FSR sensors have a continuous analog resolution and a force sensitivity range of 0.2N – 20N. Two force sensors are placed on each of the finger/thumb tip pieces, as shown in Fig. 7. The force sensors were calibrated using known weights.

In addition to the sensors, vibration motors were added to the design in order to provide feedback to the user. This feedback can be used in several applications such as, providing haptic feedback for virtual reality applications, acting as a stimulus to prompt the user to perform certain tasks for

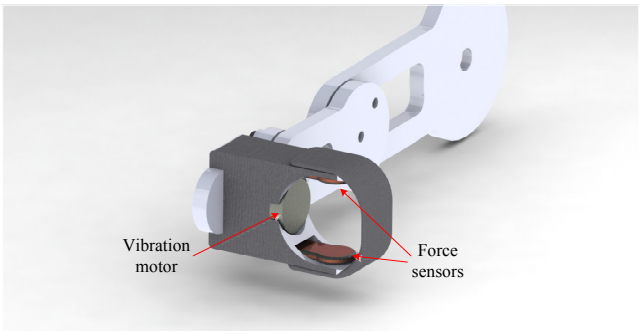

Figure 7: Detailed design of the tip holder.

rehabilitation, or as feedback for tele-navigation [3]. The motors used were Adafruit mini vibration motors, which are rated for 5V max with a current draw of 100mA. The motors have a weight of 0.9 grams and can provide a vibration sensation that resembles that of a standard mobile phone vibrating unit.

4. PROTOTYPE INTEGRATION

The basic mechanisms shown in Fig. 3 were further developed into a detailed design for the two-digit prototype. The detailed design of the system was completed in Solid Works, as shown in Fig. 1. The mechanisms for the index finger and the thumb were 3D printed separately using ABS plastic and then connected together using a base plate. The base plate, which supports the weight of the two mechanisms and the actuators, was strapped onto the back of the hand using elastic Velcro straps. This allows for the adjustment of the exoskeleton glove to suit different hand sizes. The prototype weighs 24g, making it lightweight as compared to the two finger exoskeleton of [32], which weighs 180g. To complete the prototype implementation, a circuit board and software interface were developed to control the glove and all integrated sensors. The circuit board and pneumatic system were kept separate so that they could be either incorporated into a backpack or kept on a table while the exoskeleton glove was being used.

4.1 Electrical Circuit:

A custom printed circuit board (PCB) was developed to connect the sensors and actuators with the microcontroller unit and other electrical components. The force sensors and encoders were connected to the microcontroller unit as inputs while the pneumatic actuators and vibration motors were the output connections. The pneumatic actuators were controlled using the solenoid valves to produce a linear actuation. The microcontroller itself powers these solenoid valves on/off via N-MOSFET switches. The vibration motors are directly connected to a motor driver since the current ratings of these motors exceed the tolerance of the microcontroller input/output (I/O) pins. The microcontroller connects to the motor driver with two enable pins for each vibration motors, one for the index finger and another for the thumb.

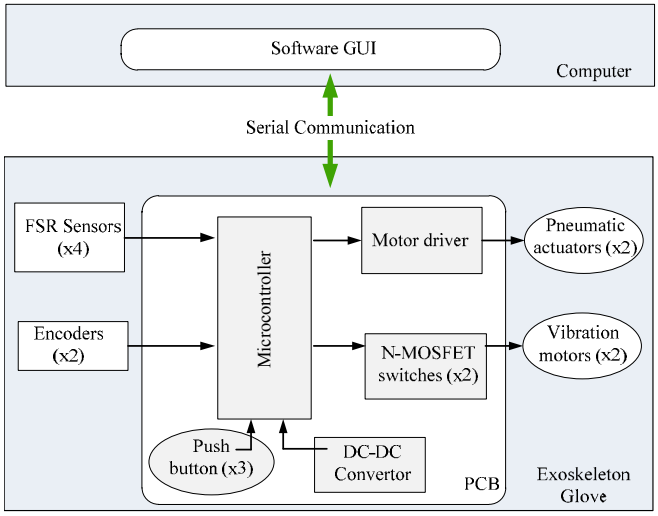

Figure 8: System architecture of exoskeleton glove.

A Teensy 3.1 board serves as the microcontroller unit for the system. It is rated at a clock frequency of 72 MHz, which provides sufficient speed for acquiring sensor data from the encoders and force sensors while performing commands to control the vibration motors and the actuation for flexion or extension of the index and thumb.

In addition to the sensors and motors, the PCB contains three tactile pushbuttons. One pushbutton serves as the main power switch while the other two are used for actuation controls. One of these two is used to depressurize the pneumatic actuators to allow free movements among the finger and thumb. The last button is used to trigger an automatic flexion and extension motion on both the finger and thumb to perform a grasp. This feature allows the exoskeleton device to serve as a standalone device for different applications such as rehabilitation. For full feature controls, the PCB can be interfaced with the Graphical User Interface (GUI) for the exoskeleton glove system that provides additional commands and functionalities. The overall architecture of the exoskeleton glove system is demonstrated in Fig. 8.

4.2 Software GUI:

The Exoskeleton GUI is an executable application developed in MATLAB. This software provides additional commands to control the glove and functionalities for data analysis. To control the glove actuation, the commands are divided into groups: index finger controls, thumb controls, and both the index finger and thumb together. Each of these control groups consist of the following commands to control only the specified finger/thumb: Trigger Motion, Release, and Vibrate Pulse. The Index and Thumb combined control group contains these same commands as well as additional commands such as the Auto Trigger and Release Pinch command, which actuates the index finger and thumb to perform a pincer grasp and then releases the pinch after a time delay of 1.50s. For all three

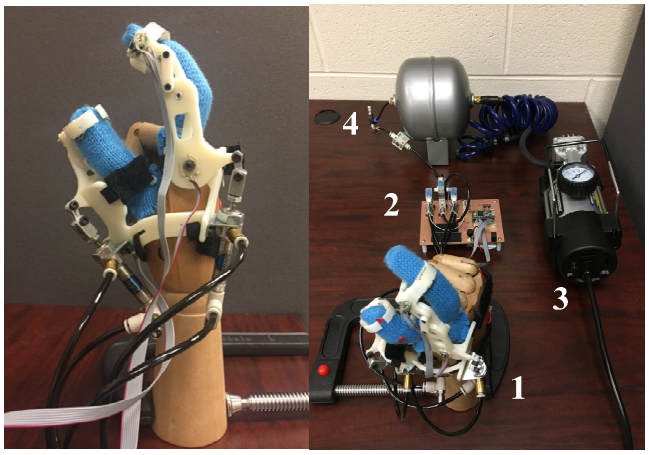

Figure 9. Experimental setup for the prototype: 1- Exoskeleton glove on mannequin, 2 - Embedded controller, 3 – Compressor, 4 - Air tank.

control groups, the Vibrate Pulse commands were programmed to turn on the corresponding vibrate motors for 0.5s.

While reading in the sensor data, the GUI displays the FSR sensor data in terms of Newtons (N) and the encoder data in degrees for both the index and thumb. For analysis purposes, the GUI has a record feature that will capture sensor data at a rate of 20Hz and store the data into a Microsoft Excel file. An additional feature of the GUI includes an imported SolidWorks CAD model of a human hand. The CAD model was incorporated to serve as a real-time animation showing the movements of the user's hand while using the glove.

5. EXPERIMENTAL VALIDATION

An experiment was conducted to verify whether the joint angles enforced on the index finger and thumb by the glove during flexions and extensions reflect the desired trajectories for obtaining natural joint coupling. The experiment involved mounting the exoskeleton glove on a wooden mannequin hand and tracking the motions of index finger and thumb, which were produced by the glove, as shown in Fig. 9. The tracking was achieved using a GoPro HERO5 Session 10MP camera with 4K video resolution. To capture the finger and thumb at various stages during motions, the camera was set up to record videos at 30 frames per seconds (FPS). A MATLAB script was programmed to utilize basic computer vision techniques to analyze the captured images. The code first identifies red markers placed on the MCP, PIP, and DIP joints and MCP and IP joints of the inserted index finger and thumb respectively. Once these red markers were identified, the centroids of the markers were computed to determine the centers of the joints. Line segments were drawn between the joint centers such that the corresponding joint angles could be calculated (illustrated in Fig. 10). Thus from identifying the red markers from image to image, the overall joint angles were calculated and used to analyze the joint coupling relationships enforced by the exoskeleton glove.

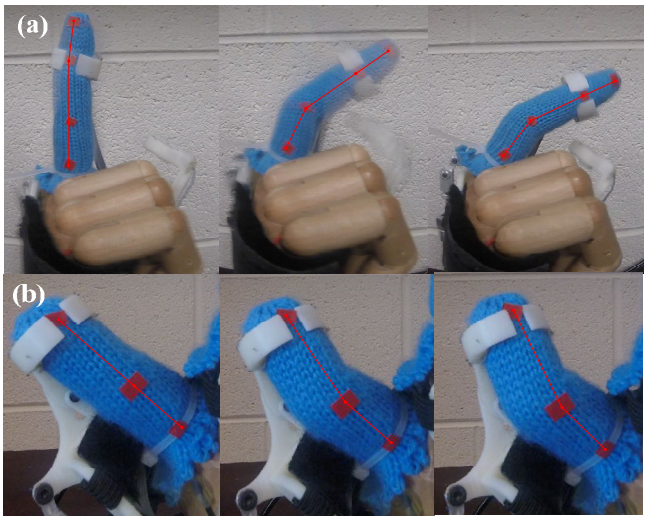

Figure 10. Experimental analysis at various stages of the bending motion: (a) Index finger, (b) Thumb

Although the GoPro camera is equipped with an ultra-wide angle lens that has reduced distortion, it was still necessary to apply a distortion correction filter to each of the video image frames prior to the joint tracking procedure. In order to accomplish this, a camera calibration was performed using the traditional method of capturing several pictures of a standard checkerboard pattern using the subject camera [33]. The distorted images of the checkerboard were then analyzed using the MATLAB camera calibration toolbox to compute the camera intrinsic, extrinsic, and lens-distortion parameters. These parameters were used for the undistortion filtering.

To overcome the lack of inherent coupling between the respective thumb and index finger joints of the mannequin hand, the index finger and thumb were inserted into a cloth glove as shown in Fig. 10. This allows for the joints to bend in correlation, when the mechanisms for index finger and thumb apply force at the distal phalange of the corresponding finger/thumb.

The experimental results are plotted in Fig. 11, displaying the calculated joint angles of the index finger and thumb with respect to time. The MCP, PIP and DIP joints of the index finger bend at average angle of 42.9°, 37.8°, and 8.01° respectively, while the MCP and IP joints of the thumb respectively bend 3.01° and 22.5°. To verify the coupling relationships of the joints, the results were compared to the targeted natural angles from [30], which were previously mentioned in Section 2. Fig. 11 displays the comparisons by plotting the resulting joint angles against the acceptable ranges of the natural joint angular displacements. More specifically, the experimentally derived upper and lower bounds for the natural joint angles for a tip-pinch force of 100g (1cm pulp distance) were computed by adding and subtracting the standard deviation with the joint angle averages [30]. These upper and lower boundaries serve as the range of acceptable variations for each of joint angle maximums.

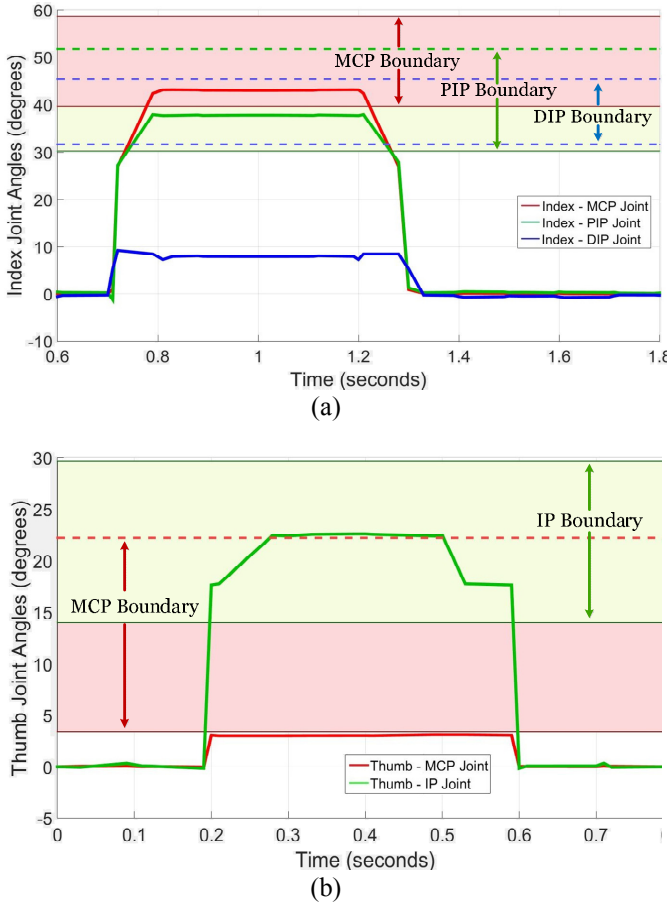

Figure 11. Experimental results for (a) Index finger joints, (b) Thumb joints

As seen from Fig. 11, the angular displacements for the MCP and PIP joints of the index finger were well within their acceptable range for natural angular displacements at the end of the pinch. However, the final angular displacement for the DIP joint of the index finger fell short from reaching within its perspective boundary by 23.7°. The MCP angular joint displacement for the thumb fell within its range while the IP joint was on the boundary of the acceptable range, falling short by 0.4°.

The shortcoming of the index finger DIP joint angle was due to the misalignment of the Velcro fingertip holder. Instead of being positioned at the distal phalange region of the mannequin hand, the holder was located near the DIP joint. This misalignment was due to the size difference between the mannequin hand and the human hand, for which the holder piece was originally designed to accommodate. The mannequin fingers were longer (index finger by 3cm and thumb by 1cm) than that of an average human hand and as a result, the mechanism was able to slide down the mannequin finger during the bending movements of the experiment. The same reason applies to the IP joint angles of the thumb coming short of the acceptable range. The glove can be seen properly worn on a human hand in Fig. 12.

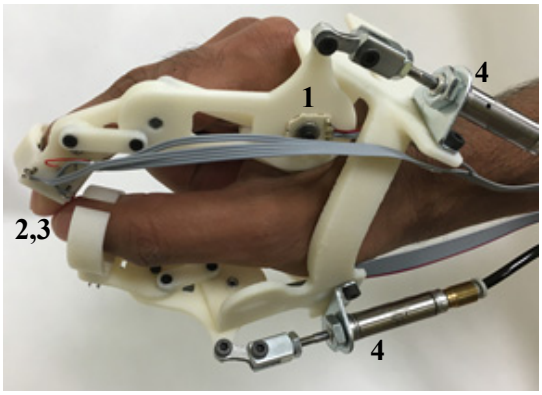

Figure 12. Prototype on a human hand: 1- Absolute position sensor, 2 – FSR sensor, 3 – Vibration motor, 4 – Pneumatic actuator.

Overall, the pincer grasp was achieved in 0.63 seconds, with 0.1 seconds for the pinch, 0.41 seconds to hold the pinch, and another 0.12 seconds for releasing. Despite the experimental shortcoming of the DIP joint of the index finger, the results demonstrated that the joint angles produced by the exoskeleton resemble natural bending trajectories of the human hand during grasping motions, such as the pincer grasp.

6. CONCLUSION & FUTURE WORK

The paper explained the design and integration of a two-digit prototype of an exoskeleton glove that was proposed to address the commonly encountered large size, heavy weight, and unnatural coupling issues of traditional hard and soft exoskeleton gloves. The design of the exoskeleton glove allows the finger and thumb mechanisms to be attached alongside the respective finger/thumb, decreasing the size of the exoskeleton glove as well as reducing the discomfort caused from using larger and heavier traditional gloves. Mathematical modeling of the design was presented and the proposed concept was validated through experiment. Results showed the potential of the exoskeleton glove to achieve natural coupling among the joints to resemble that of a human hand. The features of the prototype to record finger and thumb movements, to measure exerted forces on the glove, and to provide vibrational feedback, makes it suitable for multiple applications.

Future work involves extending the prototype into a full hand exoskeleton glove by modifying the index finger mechanism to accommodate for the additional fingers. The pneumatic actuators can be replaced with electrical actuators to improve portability and ease of use to the system as well as adding functionalities, such as force control.

ACKNOWLEDGMENTS

We would like to thank Anil Kumar of the Robotics and Mechatronics Lab at Virginia Tech for his help with this project.

REFERENCES

[1] "MANUS VR," 2014. [Online]. Available: manus-vr.com.

[2] CyberGlove Systems LLC, "CyberGrasp," 2009. [Online]. Available: http://www.cyberglovesystems.com/cybergrasp/.

[3] H. Tatsumi, Y. Murai, I. Sekita, S. Tokumasu, and M. Miyakawa, "Cane Walk in the Virtual Reality Space Using Virtual Haptic Sensing: Toward Developing Haptic VR Technologies for the Visually Impaired," *Proc. - 2015 IEEE Int. Conf. Syst. Man, Cybern. SMC 2015*, pp. 2360–2365, 2016.

[4] S. Ito, H. Kawasaki, Y. Ishigure, M. Natsume, T. Mouri, and Y. Nishimoto, "A design of fine motion assist equipment for disabled hand in robotic rehabilitation system," *J. Franklin Inst.*, vol. 348, no. 1, pp. 79–89, 2011.

[5] C. D. C. Teixeira, F. C. Marx, and J. C. De Oliveira, "A Haptic Rehabilitation System," *Proc. - 18th Symp. Virtual Augment. Reality, SVR 2016*, pp. 188–192, 2016.

[6] P. Heo, G. M. Gu, S. jin Lee, K. Rhee, and J. Kim, "Current hand exoskeleton technologies for rehabilitation and assistive engineering," *Int. J. Precis. Eng. Manuf.*, vol. 13, no. 5, pp. 807–824, 2012.

[7] Z. Ma and P. Ben-Tzvi, "Tendon transmission efficiency of a two-finger haptic glove," *ROSE 2013 - 2013 IEEE Int. Symp. Robot. Sensors Environ. Proc.*, no. October, pp. 13–18, 2013.

[8] N. S. K. Ho *et al.*, "An EMG-driven exoskeleton hand robotic training device on chronic stroke subjects: Task training system for stroke rehabilitation," *IEEE Int. Conf. Rehabil. Robot.*, 2011.

[9] J. Iqbal, H. Khan, N. G. Tsagarakis, and D. G. Caldwell, "A novel exoskeleton robotic system for hand rehabilitation - Conceptualization to prototyping," *Biocybern. Biomed. Eng.*, vol. 34, no. 2, pp. 79–89, 2014.

[10] J. Arata, K. Ohmoto, R. Gassert, O. Lambercy, H. Fujimoto, and I. Wada, "A new hand exoskeleton device for rehabilitation using a three-layered sliding spring mechanism," *Proc. - IEEE Int. Conf. Robot. Autom.*, pp. 3902–3907, 2013.

[11] T. T. Worsnopp, M. A. Peshkin, J. E. Colgate, and D. G. Kamper, "An actuated finger exoskeleton for hand rehabilitation following stroke," *2007 IEEE 10th Int. Conf. Rehabil. Robot. ICORR'07*, vol. 0, no. c, pp. 896–901, 2007.

[12] M. Takagi, K. Iwata, Y. Takahashi, S. I. Yamamoto, H. Koyama, and T. Komeda, "Development of a grip aid system using air cylinders," *Proc. - IEEE Int. Conf. Robot. Autom.*, pp. 2312–2317, 2009.

[13] I. H. Ertas, E. Hocaoglu, D. E. Barkana, and V. Patoglu, "Finger exoskeleton for treatment of tendon injuries," *Proc. 11th IEEE Int. Conf. Rehabil. Robot. ICORR*, pp. 194–201, 2009.

[14] Y. Hasegawa, Y. Mikami, K. Watanabe, and Y. Sankai, "Five-fingered assistive hand with mechanical compliance of human finger," *Proc. - IEEE Int. Conf. Robot. Autom.*, pp. 718–724, 2008.

[15] M. A. Zhou, P. Ben-Tzvi, and J. Danoff, "Hand rehabilitation learning system with an exoskeleton robotic glove," *IEEE Trans. Neural Syst. Rehabil. Eng.*, vol. PP, no. 99, pp. 1323–1332, 2015.

[16] P. Ben-Tzvi, J. Danoff, and Z. Ma, "The Design Evolution of a Sensing and Force-Feedback Exoskeleton Robotic Glove for Hand Rehabilitation Application," *J. Mech. Robot.*, vol. 8, no. 5, p. 51019, 2016.

[17] P. Ben-Tzvi and Z. Ma, "Sensing and Force-Feedback xoskeleton (SAFE) Robotic Glove," *IEEE Trans. Neural Syst. Rehabil. Eng.*, vol. 23, no. 6, pp. 992–1002, 2015.

[18] Z. Ma and P. Ben-Tzvi, "An Admittance-Type Haptic Device - RML Glove," *ASME Int. Mech. Eng. Congr. Expo.*, pp. 1–7, 2011.

[19] Z. Ma and P. Ben-Tzvi, "Design and Optimization of a Five-Finger Haptic Glove Mechanism," *J. Mech. Robot.*, vol. 7, no. 4, p. 41008, 2015.

[20] H. In and K. Cho, "Exo-Glove : Soft wearable robot for the hand using soft tendon routing system," *IEEE Robot. Autom.*, vol. 22, no. March 2015, pp. 97–105, 2015.

[21] S. W. Lee, K. A. Landers, and H. S. Park, "Development of a biomimetic hand exotendon device (BiomHED) for restoration of functional hand movement post-stroke," *IEEE Trans. Neural Syst. Rehabil. Eng.*, vol. 22, no. 4, pp. 886–898, 2014.

[22] C. J. Nycz, M. A. Delph, and G. S. Fischer, "Modeling and design of a tendon actuated soft robotic exoskeleton for hemiparetic upper limb rehabilitation," *Proc. Annu. Int. Conf. IEEE Eng. Med. Biol. Soc. EMBS*, vol. 2015–Novem, pp. 3889–3892, 2015.

[23] Y. Hasegawa, J. Tokita, K. Kamibayashi, and Y. Sankai, "Evaluation of fingertip force accuracy in different support conditions of exoskeleton," *Proc. - IEEE Int. Conf. Robot. Autom.*, pp. 680–685, 2011.

[24] I. Koo, B. Byunghyun Kang, and K.-J. Cho, "Development of Hand Exoskeleton using Pneumatic Artificial Muscle Combined with Linkage," *J. Korean Soc. Precis. Eng*, vol. 11, no. 11, pp. 1217–1224, 2013.

[25] P. Polygerinos, Z. Wang, K. C. Galloway, R. J. Wood, and C. J. Walsh, "Soft robotic glove for combined assistance and at-home rehabilitation," *Rob. Auton. Syst.*, vol. 73, pp. 135–143, 2015.

[26] K. Tadano, M. Akai, K. Kadota, and K. Kawashima, "Development of grip amplified glove using bi-articular mechanism with pneumatic artificial rubber muscle," *Proc. - IEEE Int. Conf. Robot. Autom.*, pp. 2363–2368, 2010.

[27] M. Liu and C. Xiong, "Synergistic characteristic of human hand during grasping tasks in daily life," *Lect. Notes Comput. Sci. (including Subser. Lect. Notes Artif. Intell. Lect. Notes Bioinformatics)*, vol. 8917, pp. 67–76, 2014.

[28] W. E. Hook and J. K. Stanley, "Assessment of thumb to index pulp to pulp pinch grip strengths," *J. Hand Surg. Am.*, vol. 11, no. 1, pp. 91–92, 1986.

[29] K. Hemmi, K. and Inoue, "A Proposal of Three Dimensional Movement Model for Index Finger and Thumb," *Proc. 4th Asia-Pacific Conf. Control Meas.*, 2000.

[30] A. Hara, Y. Y. Amauchi, and K. Kusunose, "Analysis of Thumb and Index Finger Joints During Pinching Motion and Writing a Cross , as Measured by Electrogoniometers," *Clin. Biomech. Relat. Res.*, pp. 282–293, 1994.

[31] G. A. Bekey, R. Tomovic, and I. Zeljkovic, "Control architecture for the Belgrade/USC Hand," *Dexterous Robot. Hands*, p. 345, 1990.

[32] Z. Ma and P. Ben-Tzvi, "RML glove-an exoskeleton glove mechanism with haptics feedback," *IEEE/ASME Trans. Mechatronics*, vol. 20, no. 2, pp. 641–652, 2015.

[33] C. Yu and Q. Peng, "Robust recognition of checkerboard pattern for camera calibration," *Opt. Eng.*, vol. 45, no. 9, p. 93201, 2006.